The Journal of Physiology

Spontaneous transient hyperpolarizations in the rabbit small intestine

Yoshihiko Kito[1,2], Masaaki Kurahashi[3], Retsu Mitsui[2], Sean M. Ward[3] and Kenton M. Sanders[3]

[1] *Department of Pharmacology, Faculty of Medicine, Saga University, Nabeshima, Saga 849-8501, Japan*
[2] *Department of Cell Physiology, Nagoya City University Medical School, Mizuho-ku, Nagoya 467-8601, Japan*
[3] *Department of Physiology and Cell Biology, University of Nevada School of Medicine, Reno, NV 89557, USA*

Key points

- Recently, it was shown that fibroblast-like cells (FLCs) possess the apparatus to mediate purinergic motor neurotransmission in the gastrointestinal tract. However, the electrophysiological properties of FLCs *in situ* have not been determined.
- We recorded two patterns of slow waves from longitudinal smooth muscle cells and circular smooth muscle cells, large amplitude slow waves from interstitial cells of Cajal, and spontaneous transient hyperpolarizations (STHs) from FLCs in the rabbit small intestine using intracellular recording combined with dye injection to identify the cellular morphology of impaled cells.
- Drugs that inhibit the signalling pathway involved in purinergic neurotransmission inhibited STHs in FLCs. Small amplitude STHs were recorded in smooth muscle cells but not in interstitial cells of Cajal, suggesting that STHs from FLCs were conducted passively to smooth muscle cells.
- We conclude that FLCs display the molecular apparatus necessary to mediate purinergic neurotransmission and may tonically dampen smooth muscle excitability in the rabbit small intestine by an ongoing discharge of STHs.

Abstract Four types of electrical activity were recorded and related to cell structure by intracellular recording and dye injection into impaled cells in muscles of rabbit small intestine. The specific cell types from which recordings were made were longitudinal smooth muscle cells (LSMCs), circular smooth muscle cells (CSMCs), interstitial cells of Cajal distributed in the myenteric region (ICC-MY) and fibroblast-like cells (FLCs). Slow waves (slow waves$_{SMC}$) were recorded from LSMCs and CSMCs. Slow waves (slow waves$_{ICC}$) were of greatest amplitude (>50 mV) and highest maximum rate of rise (>10 V s^{-1}) in ICC-MY. The dominant activity in FLCs was spontaneous transient hyperpolarizations (STHs), with maximum amplitudes above 30 mV. STHs were often superimposed upon small amplitude slow waves (slow waves$_{FLC}$). STHs displayed a cyclical pattern of discharge irrespective of background slow wave activity. STHs were inhibited by MRS2500 (3 μM), a P2Y1 antagonist, and abolished by apamin (0.3 μM), a blocker of small conductance Ca^{2+}-activated K^+ channels. Small amplitude STHs (<15 mV) were detected in smooth muscle layers, whereas STHs were not resolved in cells identified as ICC-MY. Electrical field stimulation evoked purinergic inhibitory junction potentials (IJPs) in CSMCs. Purinergic IJPs were not recorded from ICC-MY. These results suggest that FLCs may regulate smooth muscle excitability in the rabbit small intestine via generation of rhythmic apamin-sensitive STHs. Stimulation of P2Y1 receptors modulates the amplitudes of STHs. Our results also suggest that purinergic inhibitory motor neurons regulate the motility of the rabbit small intestine by causing IJPs in FLCs that conduct to CSMCs.

DOI: 10.1113/jphysiol.2014.276337

(Received 22 April 2014; accepted after revision 1 September 2014; first published online 5 September 2014)
Corresponding author Y. Kito: Department of Pharmacology, Faculty of Medicine, Saga University, Nabeshima, Saga, 849-8501, Japan. E-mail: ykito@cc.saga-u.ac.jp

Abbreviations CSMC, circular smooth muscle cell; DMP, deep muscular plexus; EFS, electrical field stimulation; EJP, excitatory junction potential; FLC, fibroblast-like cell; GI, gastrointestinal; ICC, interstitial cells of Cajal; IJP, inhibitory junction potential; L-NNA, N^{ω}-nitro-L-arginine; LSMC, longitudinal smooth muscle cell; ODQ, ^{1}H [1,2,4] oxadiazolo [4,3-a]quinoxalin-1-one; PDGFRα, platelet-derived growth factor receptor α; P2Y1, purinergic receptor P2Y1; STH, spontaneous transient hyperpolarization.

Introduction

Interstitial cells of Cajal (ICC) are distributed throughout the gastrointestinal (GI) tract from smooth muscle portions of the oesophagus through the internal anal sphincter in organ-specific, stereotypical patterns in mammals (Thuneberg, 1982; Sanders, 1996; Komuro *et al.* 1999; Komuro, 2006). In stomach, small bowel and colon, an interconnected network of ICC lies with the myenteric region (ICC-MY) and provides pacemaker activity, generating electrical slow waves (slow waves$_{ICC}$) that time the phasic contractions in these organs (Ward *et al.* 1994; Huizinga *et al.* 1995). Intramuscular interstitial cells of Cajal (ICC-IM) lie within muscle bundles and participate in the transduction of neurotransmitter signals from enteric motor neurons (Burns *et al.* 1996; Ward & Sanders, 2006; Duffy *et al.* 2012). ICC loss has been associated with several GI motility disorders, such as gastroparesis, chronic idiopathetic intestinal pseudoobstraction and inflammatory bowel disease (Sanders *et al.* 1999; Vanderwinden *et al.* 1999; Burns, 2007; Farrugia, 2008). Major advances in understanding the role of ICC in GI motility came from studies of *W/W^{v}* mice and *W/Ws* rats that have reduced ICC in many organs (Ward *et al.* 1994; Huizinga *et al.* 1995; Burns *et al.* 1996; Sanders, 1996).

Interestingly, *W* mutants shed light on another, c-Kit-negative, type of interstitial cell in the GI tract, referred to as fibroblast-like cells (FLCs) (Horiguchi & Komuro, 2000; Iino & Nojyo, 2009; Sanders *et al.* 2010). FLCs are found in approximately the same anatomical niches as ICC (e.g. in the myenteric region and lying in close proximity to nerve terminals of enteric neurons within muscle bundles). FLCs form gap junctions with surrounding smooth muscle cells (SMCs) in wild-type (WT) and *W/W^{v}* mice (Horiguchi & Komuro, 2000). Immunohistochemical studies indicate that small conductance Ca^{2+}-activated K^{+} (SK3) channel protein, a potential mediator of purinergic enteric hyperpolarization and inhibition of contractions, is expressed in FLCs but not in SMCs or ICC in the small intestine (Klemm & Lang, 2002; Vanderwinden *et al.* 2002; Fujita *et al.* 2003; Iino & Nojyo, 2009). Furthermore, apamin-sensitive inhibitory junction potentials (fIJPs) were detected in the gastric fundus or antrum of *W/W^{v}* mice (Burns *et al.* 1996; Suzuki *et al.* 2003). These results raised the possibility that FLCs may be involved in the purinergic inhibitory neurotransmission of the GI tract.

FLCs are selectively labelled by and distinguished from other types of cells in the tunica muscularis in mice (Iino *et al.* 2009; Kurahashi *et al.* 2011; Cobine *et al.* 2011) and human colon (Kurahashi *et al.* 2012) with antibodies against platelet derived growth factor receptor α (PDGFRα). PDGFRα^{+} cells isolated from the mouse colon display apamin-sensitive outward currents that are activated by P2Y1 agonists, and outward currents could not be resolved in SMCs under physiological gradients and holding potentials (Kurahashi *et al.* 2011). These results suggest that PDGFRα^{+} cells could be targets for purinergic motor neurotransmission in the GI tract. However, the behaviour of FLCs *in situ* has not previously been recorded, and thus the contribution of these cells to regulation of smooth muscle excitability in GI muscles has not been measured directly. In this study we recorded directly from FLCs *in situ* with intracellular microelectrodes and showed these cells generated spontaneous transient hyperpolarizations (STHs) in the rabbit small intestine. We filled cells with fluorescent dyes while recording to relate cellular morphology with specific electrical behaviours. Our data suggest that FLCs provide a net inhibitory influence and may contribute to tonic inhibition, a previously described motor pattern of GI muscles (Wood, 1972; Waterman & Costa, 1994; Spencer *et al.* 1998). Some of the results were reported briefly at a Joint International Neurogastroenterology and Motility Meeting (Kito, 2012).

Methods

Tissue preparations

Male Japanese albino rabbits, weighing 2–2.5 kg, were anaesthetized by injection of pentobarbitone sodium (50 mg kg^{-1}, given I.V.), then killed by exsanguination. Maintenance of animals and all experimental protocols involving animals were performed in accordance with the Guidelines for the Care and Use of Laboratory Animals of Nagoya City University Medical School and accredited by The Physiological Society of Japan. All procedures were approved by Nagoya City University Animal Center (approval No.H18M-31). Segments of terminal ileum were removed from animals and opened along the mesenteric

border, in Krebs solution (see below). The mucosal and the serosal layers were carefully removed under a dissecting microscope. A tissue segment (about 1 × 1 mm^2) was pinned out on a silicone rubber plate with the longitudinal side uppermost, and the plate was fixed at the bottom of an organ bath (8 mm wide, 8 mm deep, 20 mm long). The tissue was superfused with warmed (35°C) and oxygenated Krebs solution, at a constant flow rate of approximately 2 ml min^{-1}. Experiments were carried out in the presence of 3 μM nifedipine throughout, and this minimized the movement of muscles.

Electrophysiological recording

Conventional microelectrode techniques were used to record intracellular electrical activity from smooth muscle tissues, and the glass capillary microelectrodes (outer diameter 1.5 mm, inner diameter 0.86 mm; Hilgenberg, Malsfeld, Germany) filled with 2 M KCl had tip resistances ranging between 50 and 80 MΩ. Electrical responses recorded via a high input impedance amplifier (Axoclamp-2B; Axon Instruments, Foster City, CA, USA) were displayed on a cathode-ray oscilloscope (SS-7602; Iwatsu, Osaka, Japan) and stored on a computer for subsequent analysis and display.

Cellular impalements were made with microelectrodes filled with 2 M KCl and 0.5% (w/v) propidium iodide (PI; Sigma, St Louis, MO, USA) to identify the morphological features of cells in the ileum. Impaled cells were filled with PI by passing hyperpolarizing current pulses (duration 100 ms, intensity 1 nA, frequency 3 Hz for 5–30 min) supplied from an electric stimulator (SEN-3301; Nihon Kohden, Tokyo, Japan) (Kito *et al.* 2009). After filling cells, the muscles were fixed overnight at 4°C with fresh 4% (w/v) paraformaldehyde in 0.1 M PBS. After fixation, the muscles were washed several times with PBS, mounted in DAKO fluorescent mounting medium (DAKO Corp., Carpinteria, CA, USA), covered with a coverslip and viewed with a confocal microscope (LSM5 PASCAL; Carl Zeiss, Göttingen, Germany). The confocal microscope with a krypton–argon laser allowed the visualization of PI (488 nm excitation filter and 560 nm emission long pass filter).

Electrical stimulation of the intramural nerves was achieved with a silver wire (diameter 0.3 mm) coated with enamel, except at the tip, and placed above the tissue, and a second electrode (silver plate) placed in the bath (i.e. the point stimulating method). Brief current pulses (0.3 ms, 10 pulses at 50 Hz, supra-optimal voltage) were applied to the stimulating electrodes, by an electric stimulator.

Statistics

Experimental values were expressed by the mean value ± SD. Statistical significance was tested using Student's *t* test, and probabilities of less than 5% ($P < 0.05$) were considered significant.

Solutions and drugs

The ionic composition of the Krebs solution was as follows (mM): Na^+, 137.4; K^+, 5.9; Ca^{2+}, 2.5; Mg^{2+}, 1.2; HCO_3^-, 15.5; $H_2PO_4^-$, 1.2; Cl^-, 134; and glucose, 11.5. The solutions were aerated with O_2 containing 5% CO_2, and the pH of the solutions was maintained at 7.2–7.3.

Drugs used were apamin, ω-conotoxin GVIA (from Peptide Institute, Osaka, Japan), atropine sulphate, nifedipine, N^{ω}-nitro-L-arginine (L-NNA) (all from Sigma), MRS2500 and ^{1}H [1,2,4] oxadiazolo [4,3-a]quinoxalin-1-one (ODQ) (from Tocris Cookson, Bristol, UK), and TTX (from Wako, Osaka, Japan). Nifedipine and ODQ were dissolved in DMSO to make stock solutions, and were added to Krebs solution to make the desired concentrations, just prior to use. All other drugs were dissolved first in distilled water. The final concentration of the solvent in Krebs solution did not exceed 1:1000. Addition of these chemicals to Krebs solution did not alter the pH of the solution.

Results

Identification of spontaneous active cells in the rabbit small intestine

The first cells impaled in strips of rabbit small intestine with the longitudinal layer facing upward had resting membrane potentials (RMPs) of −45 mV (Table 1) and displayed spontaneous slow wave activity (Fig. 1*A*). Slow waves in these cells had peak amplitudes of 6–15 mV, maximum rate of rise (dV/dt_{max}) of less than 0.3 V s^{-1} and half-widths of 2–3 s, measured at 50% peak amplitude. By filling with PI (0.5%, w/v) while recording, we determined that the peripheral cells with slow wave activity were long and narrow, and the long axis of the cells was orientated along the longitudinal axis of the small intestine. Thus, these cells were identified as longitudinal smooth muscle cells (LSMCs) (Fig. 1*B*).

If the electrode was advanced through the longitudinal layer, cells with different electrical behaviours were typically impaled (Fig. 1*C*). These cells displayed slow waves that had peak amplitudes of 18–30 mV and dV/dt_{max} of less than 0.5 V s^{-1} (Table 1). These cells had RMPs of about −64 mV (Table 1). The shape and orientation of those cells identified them as circular smooth muscle cells (CSMCs; Fig. 1*D*). In rare instances (<1% of all cells impaled) electrodes advanced through the longitudinal layer impaled cells that generated large amplitude slow waves (Fig. 2*A*). These cells had peak amplitudes of

Table 1. Properties of electrical active cells recorded from the rabbit small intestine

	Resting membrane potential (mV)	Amplitude (upstroke) (mV)	Amplitude (plateau) (mV)	Frequency (min^{-1})	Half-width (s)	dV/dt_{max} ($V\ s^{-1}$)	*n*
LSMC	−44.8 ± 3.9		9.1 ± 2.5	10.1 ± 1.5	2.6 ± 0.4	0.2 ± 0.1	20
CSMC	−63.5 ± 2.4		24.4 ± 2.7	10.6 ± 1.7	2.3 ± 0.4	0.4 ± 0.1	38
ICC-MY	−65.1 ± 2.8	56.9 ± 6.4	49.7 ± 4.5	10.2 ± 1.1	2.4 ± 0.3	10.6 ± 3.4	10
FLCs	−49.5 ± 5.3		14.4 ± 4.7	10.1 ± 0.1	2.3 ± 0.5	0.4 ± 0.1	12

Values are means ± SD. *n* = number of animals.

49–71 mV, dV/dt_{max} of 7–17 V s^{-1} and RMPs of about −65 mV (Table 1). These cells had triangular cell bodies with multiple long, thin processes (Fig. 2*B*) (Cajal, 1911; Thuneberg, 1982; Komuro *et al.* 1999). These results suggest that large amplitude slow waves were recorded from ICC-MY.

In still fewer cases (<0.1% of cells), when the electrodes were advanced through the longitudinal muscle layers, cells with quite different electrical properties were impaled (Fig. 3*A*). These cells were characterized by RMPs of about −50 mV, large amplitude negative deflections in membrane potential (STHs), and slow wave activity averaging 9–20 mV in amplitude and with dV/dt_{max} of less than 0.5 V s^{-1} (Table 1). STHs were observed during the intervals between slow waves or superimposed upon any phase of the slow waves (Fig. 3*A*). These cells lay close to the region of the myenteric plexus as any region, because any further downward movement of the electrode tip invariably led to impalements of ICC-MY or, more typically, SMCs (data not shown). Cells with STHs had morphologies that differed from SMCs and ICC-MY; STH cells were irregular in shape and possessed multiple processes of varying length (Fig. 3*B*). Networks of ICC-MY or cells with STHs have never been identified even if PI was injected for a long period of time (>30 min). All types of slow waves occurred at the same frequency

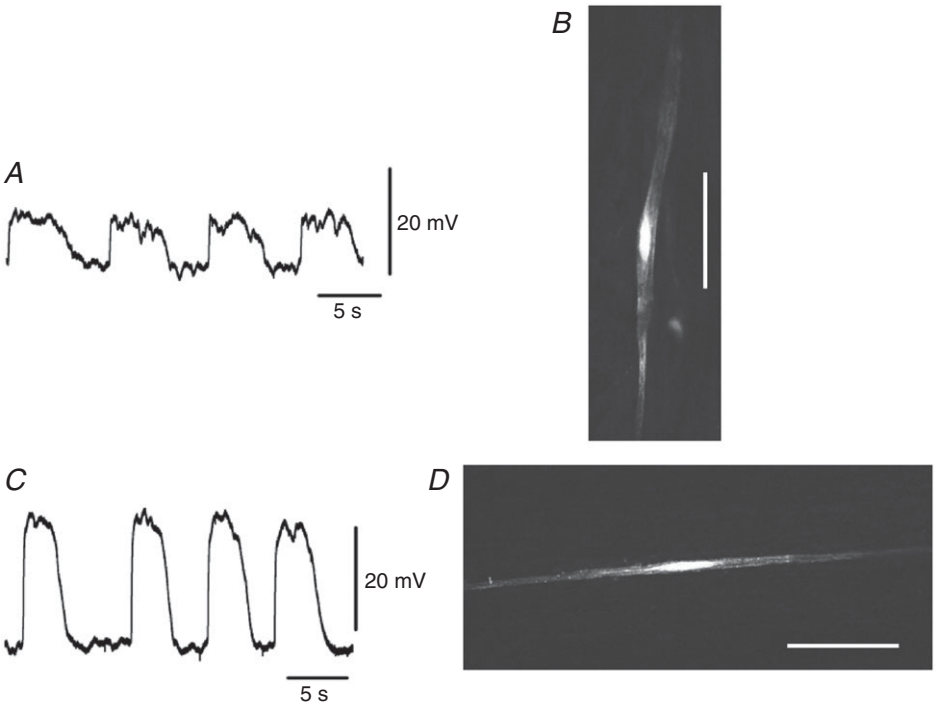

Figure 1. Morphological features of cells with slow waves filled with propidium iodide
A, slow waves recorded from a cell in the longitudinal layer shown in *B*. The shape of the cell injected with propidium iodide for 5 min was digitally reconstructed on a confocal microscope (*B*). *C*, slow waves recorded from a cell in the circular layer shown in *D*. The shape of the cell injected with propidium iodide for 5 min was digitally reconstructed on a confocal microscope (*D*). Cells in *B* and *D* are of the general morphology of SMCs in the longitudinal and circular muscle layers. The scale bars in *B* and *D* represent 50 μm. The resting membrane potentials were: *A*, −46 mV; *C*, −64 mV. *A* and *C* were recorded from different tissues.

(about 10 min^{-1}) in each muscle preparation (Table 1), and nifedipine (3 μM) had little effect on any of the types of electrical activities observed.

Properties of STHs recorded from cells with STHs

Figure 4*A* shows typical STHs recorded from cells impaled beneath the longitudinal muscle cells. Since constant generation of STHs (>10 mV) has never been recorded from SMCs (see Fig. 8), cells with STHs (>10 mV) that occurred constantly were analysed as FLCs. STHs ranged between 4.2 and 34.2 mV in amplitude. STH amplitudes followed a Gaussian distribution, and STHs had most events that were 17.5 mV in amplitude (Fig. 4*B*). The amplitude of STHs increased during slow waves, probably because slow waves drive membrane potential away from E_K (Fig. 4*C*). STHs were generated at frequencies of 24–60 min^{-1} (43.3 ± 13.5 min^{-1}; $n = 8$). Interestingly, in four preparations, the amplitude and frequency of STHs varied with time, as shown in Fig. 5. The frequency of STHs decreased from 37.3 ± 5.8 to 20.8 ± 11.9 min^{-1} ($n = 4$; $P < 0.05$), and increased again to 36.3 ± 4.1 min^{-1} ($n = 4$; $P > 0.05$) during a 6–23 min recording in which there were no changes in the background slow wave activity (Fig. 5). The duration of the cyclical attenuation of STHs was 2.2 ± 0.8 min^{-1} ($n = 4$). The morphological characteristics and ongoing STHs suggest that the cells with STHs were FLCs, given that isolated FLCs display spontaneous transient outward currents (Kurahashi *et al.* 2011).

P2Y1 agonists activate large amplitude Ca^{2+}-activated apamin-sensitive outward currents in FLCs (PDGFRα^+ cells) from the murine colon (Kurahashi *et al.* 2011). Therefore, we tested the effects of MRS2500, an antagonist of P2Y1 receptors, and apamin on STHs. Application of MRS2500 (3 μM) depolarized cells by 8.5 ± 2.3 mV ($n = 3$) and decreased the amplitude (11.2 ± 4.7 to 2.9 ± 1.1 mV; $n = 3$; $P < 0.01$) and frequency (40.1 ± 9.8 to 21.3 ± 3.2 min^{-1}; $n = 3$; $P < 0.01$) of STHs in MRS2500 (Fig. 6*A*). Residual STHs in the presence of MRS2500 were abolished by co-application of apamin (0.3 μM) ($n = 2$; data not shown). Apamin alone (0.3 μM) depolarized FLCs by 9.5 ± 1.7 mV ($n = 4$) and abolished STHs (Fig. 6*B*). Application of 3 μM TTX had no effect on the RMP (−42.0 ± 4.5 to −40.3 ± 5.9 mV; $n = 4$; $P > 0.05$), amplitude (18.5 ± 2.2 to 17.6 ± 2.5 mV; $n = 4$; $P > 0.05$) or frequency (44.5 ± 3.8 to 41.8 ± 7.8 min^{-1}; $n = 4$; $P > 0.05$) of STHs (Fig. 7*A*). Similarly, 0.5 μM ω-conotoxin

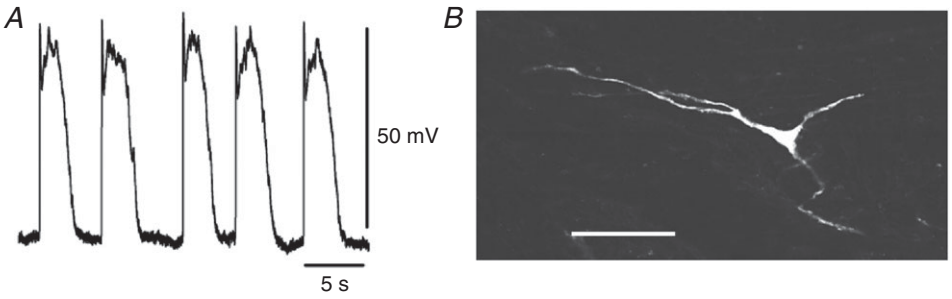

Figure 2. Morphological features of cells with large amplitude slow waves filled with propidium iodide
A, slow waves recorded from the cell shown in *B*. The resting membrane potential was −65 mV. The image of the cell injected with propidium iodide for 4 min was digitally reconstructed on a confocal microscope, and it shows the distinctive morphology of an ICC-MY (*B*). The scale bar *B* in represents 50 μm.

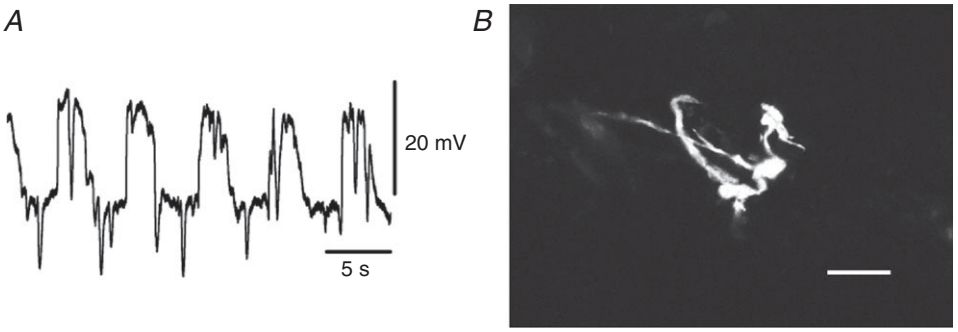

Figure 3. Morphological properties of cells with STHs filled with propidium iodide
A, STHs recorded from a cell in the region between the circular and longitudinal muscle layers shown in *B*. The resting membrane potential was −43 mV. The shape of the cell injected with propidium iodide for 20 min was digitally reconstructed on a confocal microscope, and this morphology is consistent with this cell being an FLC (*B*). The scale bar in *B* represents 50 μm.

GVIA (ω-Ctx) had no effect on the RMP (-44.7 ± 4.6 to -45.3 ± 8.1 mV; $n = 3$; $P > 0.05$), amplitude (19.8 ± 6.6 to 20.3 ± 9.1 mV; $n = 3$; $P > 0.05$) or frequency (32.2 ± 5.2 to 31.9 ± 7.5 min^{-1}; $n = 3$; $P > 0.05$) of STHs (Fig. 7*B*). These results suggest that STHs occur basically by spontaneous activation of SK channels in FLCs. The P2Y1 signalling pathway appears to augment ongoing STHs, but the natural agonist stimulating P2Y1 receptors appears to come from a TTX-resistant mechanism. Sensitivity of STHs to apamin and MRS2500 is consistent with these cells being FLCs, as the spontaneous transient outward currents in these cells are also sensitive to these blockers (Kurahashi *et al.* 2011).

Properties of STHs recorded from SMCs

STHs were also observed in SMCs (<30% of all LSMCs impaled and <3% of all CSMCs impaled). Figure 8*A*

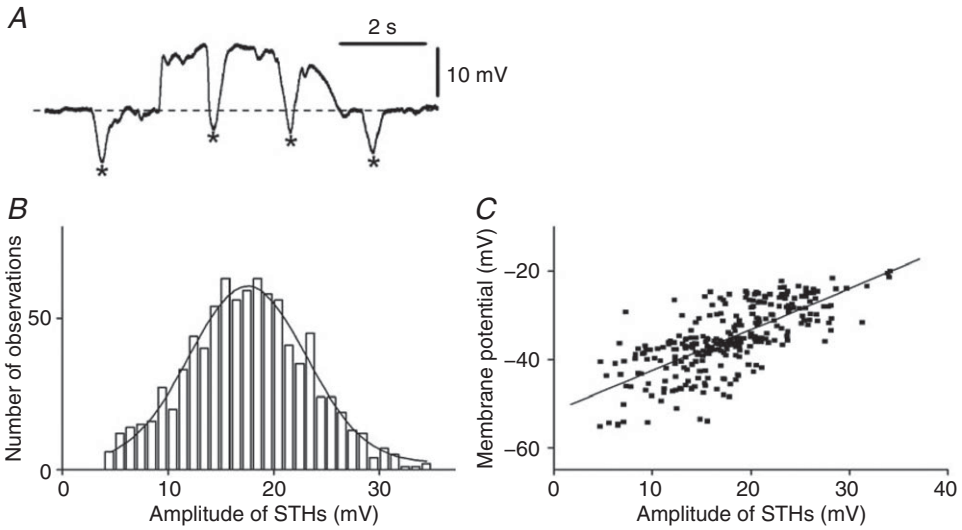

Figure 4. Properties of STHs recorded from fibroblast-like cells of rabbit small intestine
A, a train of STHs superimposed upon a slow wave depolarization recorded from a fibroblast-like cell. The asterisks indicate individual STHs in the trace. Note that STHs occurred during and between slow wave depolarizations. *B*, amplitude histogram of STHs recorded from fibroblast-like cells. The curve is a Gaussian distribution, with a mean of 17.5 mV and standard deviation of 0.2 mV. *C*, relationship between the amplitude of STHs and membrane potential just prior to the generation of STHs. The regression line is given by $y = 0.73x - 51.8$ ($r = 0.63$; $n = 869$ from 8 preparations, $P < 0.001$).

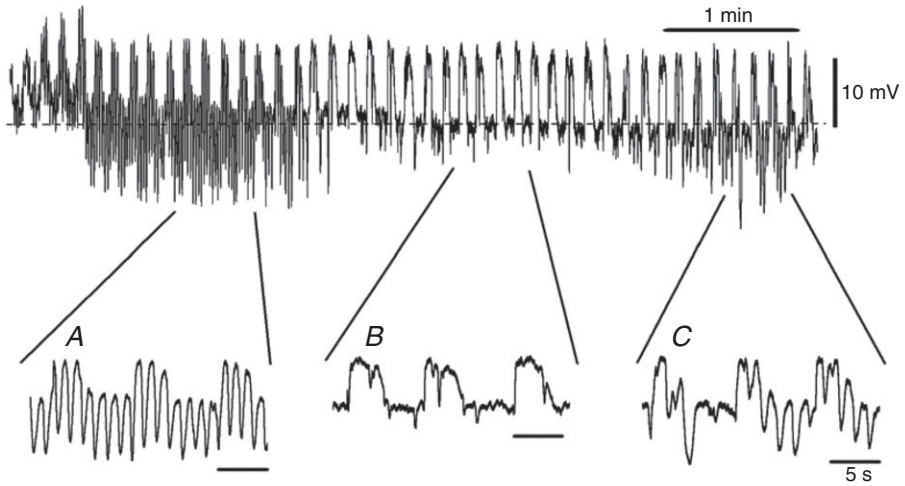

Figure 5. Periodical changes in STHs in rabbit small intestine
Train of STHs for 6 min. The pattern of STH discharge changed as a function of time. In this example the frequency and amplitude of STHs changed, as displayed in the excerpts shown below the main trace: *A*, 47 min^{-1}; *B*, 40 min^{-1}; *C*, 43 min^{-1}. The resting membrane potential of this cell was −51 mV.

and *C* shows examples of STHs recorded from LSMCs and CSMCs, respectively. Therefore, to examine the amplitude/frequency histogram, amplitudes >1 mV were measured. STH amplitudes detected in LSMCs ranged from 1.1 to 16.4 mV (Fig. 8*B*). However, STHs having amplitudes of more than 10 mV were not generated constantly. The distribution of STH amplitude detected in CSMCs ranged from 1.1 to 8.8 mV (Fig. 8*D*). These results indicate that the amplitudes of STHs were far smaller in SMCs than in FLCs. STHs observed in SMCs were all abolished by apamin (0.3 μM). In contrast to SMCs, STHs were never observed in ICC-MY.

Properties of purinergic neurotransmission in the circular layers

It has been reported that IJPs in the circular layer evoked by the activation of enteric inhibitory motor neurons consisit of a fast purinergic IJP (fIJP) followed by a slower nitrergic IJP (sIJP) in the small intestine (Stark *et al.* 1991; Crist *et al.* 1992; He & Goyal, 1993). Recent studies have demonstrated that P2Y1 receptors are responsible for fIJP in the small intestine (Wang *et al.* 2007; Gallego *et al.* 2008; Hwang *et al.* 2012). Therefore, in the next series of experiments, the mechanisms of generation of fIJP in the rabbit small intestine were compared with those of

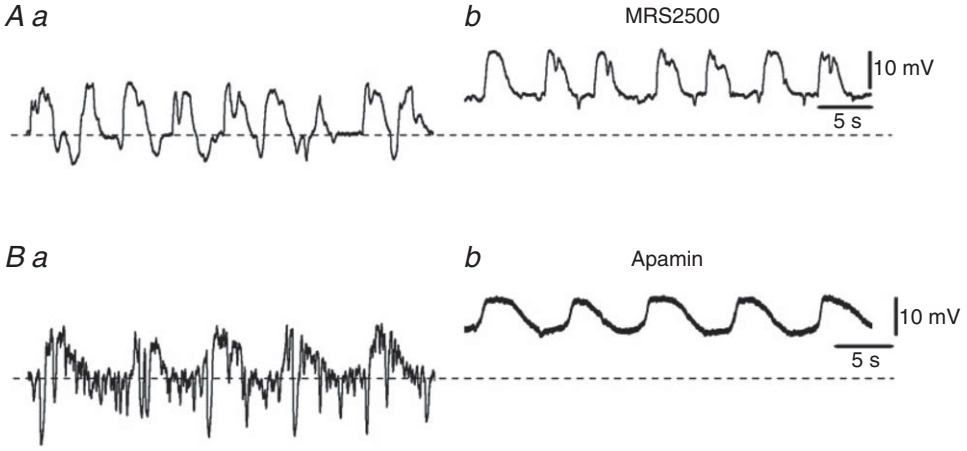

Figure 6. Effects of MRS2500 and apamin on STHs recorded from rabbit small intestine
A, STHs were recorded before (*Aa*) and during application of 3 μM MRS2500 (*Ab*). *B*, STHs were recorded before (*Ba*) and during application of 0.3 μM apamin (*Bb*). The resting membrane potentials were: *A*, −59 mV; *B*, −48 mV. *A* and *B* were recorded from different tissues.

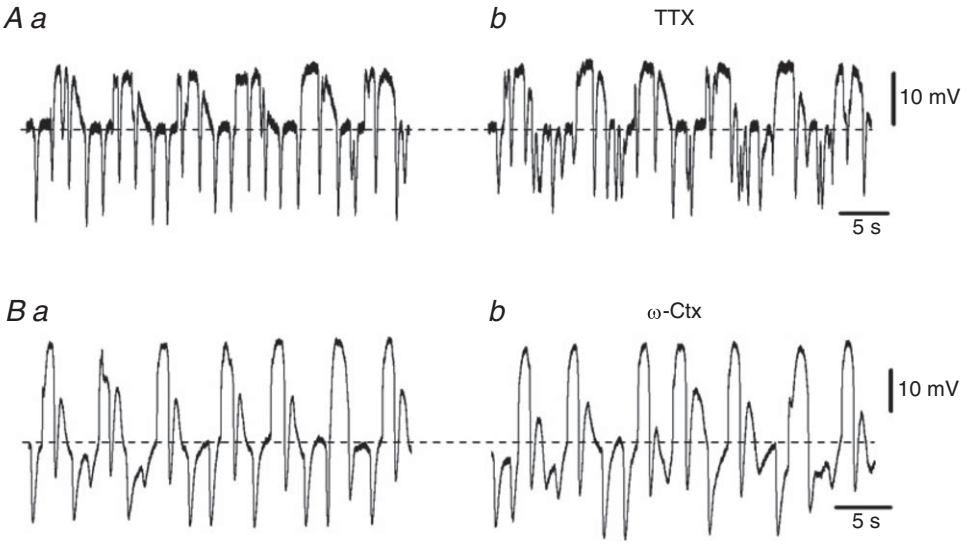

Figure 7. Effects of TTX and ω-conotoxin GVIA on STHs recorded from rabbit small intestine
A, STHs were recorded before (*Aa*) and during application of 3 μM TTX (*Ab*). *B*, STHs were recorded before (*Ba*) and during application of 0.5 μM ω-conotoxin GVIA (ω-Ctx) (*Bb*). The resting membrane potentials were: *A*, −41 mV; *B*, −43 mV. *A* and *B* were recorded from different tissues.

STHs recorded from FLCs. To assess the properties of fIJP in the rabbit small intestine, the effects of electrical field stimulation (EFS) on electrical activity recorded from CSMCs were studied in the presence of atropine (3 μM) and L-NNA (100 μM). Application of EFS (0.3 ms; 10 pulses at 50 Hz; supra-optimal voltage) during the intervals between slow waves recorded from CSMCs generated a hyperpolarizing response followed by an increase in slow wave duration (Fig. 9*Aa*). TTX (1 μM) abolished all responses to EFS ($n = 4$), indicating that intrinsic nerves evoked these responses. IJPs in the presence of atropine and L-NNA were converted to excitatory junction potentials (EJPs) in the presence of MRS2500 (3 μM) (control, -9.0 ± 1.5 mV; in MRS2500, 17.9 ± 1.9 mV; $n = 6$; $P < 0.01$) (Fig. 9*Ab*), suggesting that fIJP is caused by purinergic inhibitory responses via P2Y1 receptors in the circular layer of the rabbit small intestine. When EFS was applied at the peak of slow waves recorded from CSMCs,

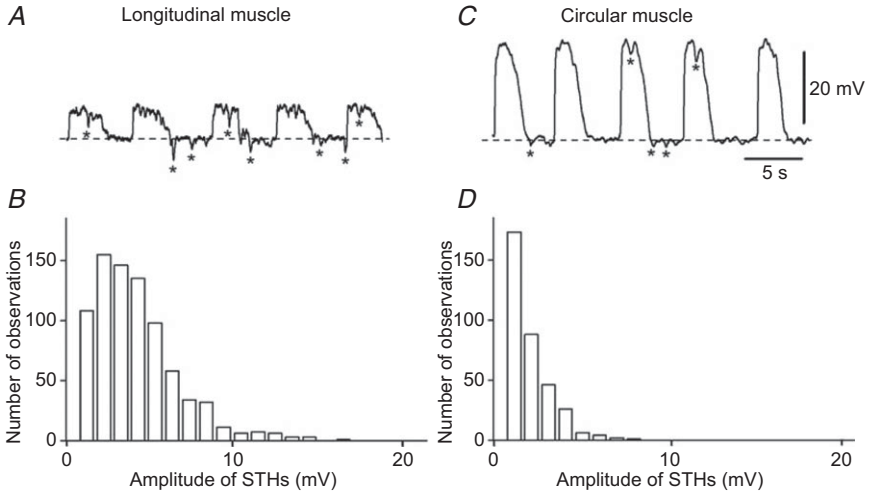

Figure 8. Properties of STHs recorded from smooth muscle cells of rabbit small intestine
A, a train of STHs recorded from a longitudinal muscle cell. *B*, amplitude histogram of STHs recorded from longitudinal muscles; $n = 806$ from 8 preparations. *C*, a train of STHs recorded from a circular muscle cell. *D*, amplitude histogram of STHs recorded from circular muscles; $n = 346$ from 8 preparations. The asterisks indicate individual STHs in each trace.

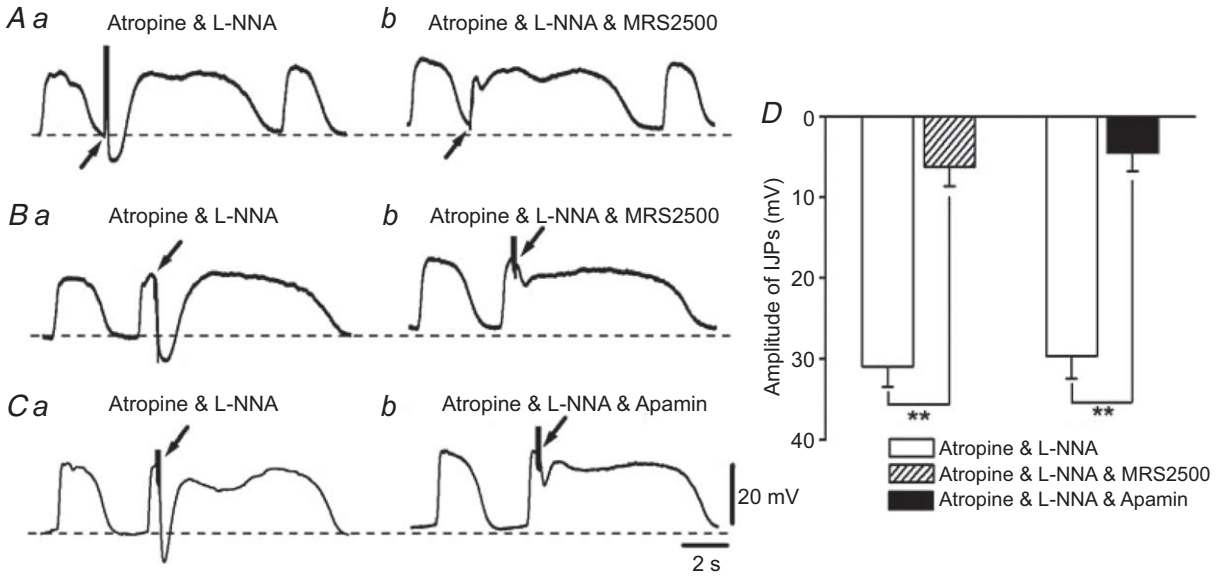

Figure 9. Effects of MRS2500 and apamin on inhibitory junction potentials evoked by electrical field stimulation recorded from circular smooth muscle cells of rabbit small intestine
A, IJPs were evoked during the intervals between slow waves recorded from circular smooth muscle cells (CSMCs) before (*Aa*) and after application of 3 μM MRS2500 (*Ab*). *B*, IJPs were evoked at the peak of slow waves recorded from CSMCs before (*Ba*) and after application of 3 μM MRS2500 (*Bb*). *C*, IJPs were evoked at the peak of slow waves recorded from CSMCs before (*Ca*) and after application of 0.3 μM apamin (*Cb*). *D*, summary of the effects of MRS2500 (3 μM) or apamin (0.3 μM) on IJPs evoked at the peak of slow waves recorded from CSMCs in the presence of atropine and L-NNA. The resting membrane potentials were: *A*, −62 mV; *B*, −62 mV; *C*, −64 mV. Atropine (3 μM) and L-NNA (100 μM) were present throughout. Scale bars on the electrical traces in *C* apply to all traces. All traces were recorded from different tissues. Data are means ± SD. $^{**}P < 0.01$, significant difference from control.

IJPs with large amplitudes (>20 mV) were generated (Fig. 9*Ba*, *Ca* and *D*). MRS2500 (3 μM) inhibited fIJP to the level found in the presence of apamin (0.3 μM) (Fig. 9*Bb*, *Cb* and *D*) ($n = 9$ for MRS2500; $n = 7$ for apamin), indicating that fIJPs in the rabbit small intestine were mediated by P2Y1 receptors through a pathway that involves activation of SK channels.

EFS-induced responses in ICC-MY

It has been demonstrated that ICC-MY are not innervated directly by inhibitory nerves in the guinea pig gastric antrum (Dickens *et al.* 2000). However, it is unclear if this is the case for all ICC-MY in other regions of the GI tract. Thus, attempts were made to study the effects of EFS on electrical activity recorded from ICC-MY in the rabbit small intestine. EFS applied at the plateau component of slow waves$_{ICC}$ caused a prolongation in slow waves$_{ICC}$ duration in the presence of atropine (3 μM) and L-NNA (100 μM) (Fig. 10*Aa*). In the presence of TTX (1 μM), EFS did not evoke any detectable change in slow waves$_{ICC}$ (Fig. 10*Ab*). When EFS was applied during the intervals between slow waves$_{ICC}$, a rapid depolarization was generated, which was followed by the enhancement of the duration of slow waves$_{ICC}$ (Fig. 10*B*). These results suggest that ICC-MY of the rabbit small intestine receive little functional innervation from purinergic inhibitory neurons. In the absence of L-NNA, application of EFS at the plateau component of slow waves$_{ICC}$ produced IJP-like responses followed by an increase in slow waves$_{ICC}$ duration (Fig. 10*Ca*). Generation of those IJP-like responses was inhibited by L-NNA (100 μM) ($n = 6$; $P < 0.01$) or ODQ (10 μM) ($n = 4$; $P < 0.01$), the latter an inhibitor of soluble guanylate cyclase (Fig. 10*Cb*, *D*), indicating that ICC-MY of the rabbit small intestine may receive functional innervation from nitrergic inhibitory nerves (Sanders & Ward, 1992; Ward *et al.* 1992). EFS-induced potentiation in the duration of slow waves$_{ICC}$ may result from the release of excitatory neurotransmitters. However, this excitatory phenomenon has not been examined further.

Discussion

In the rabbit small intestine, four types of electrically active cells were identified by intracellular recording combined

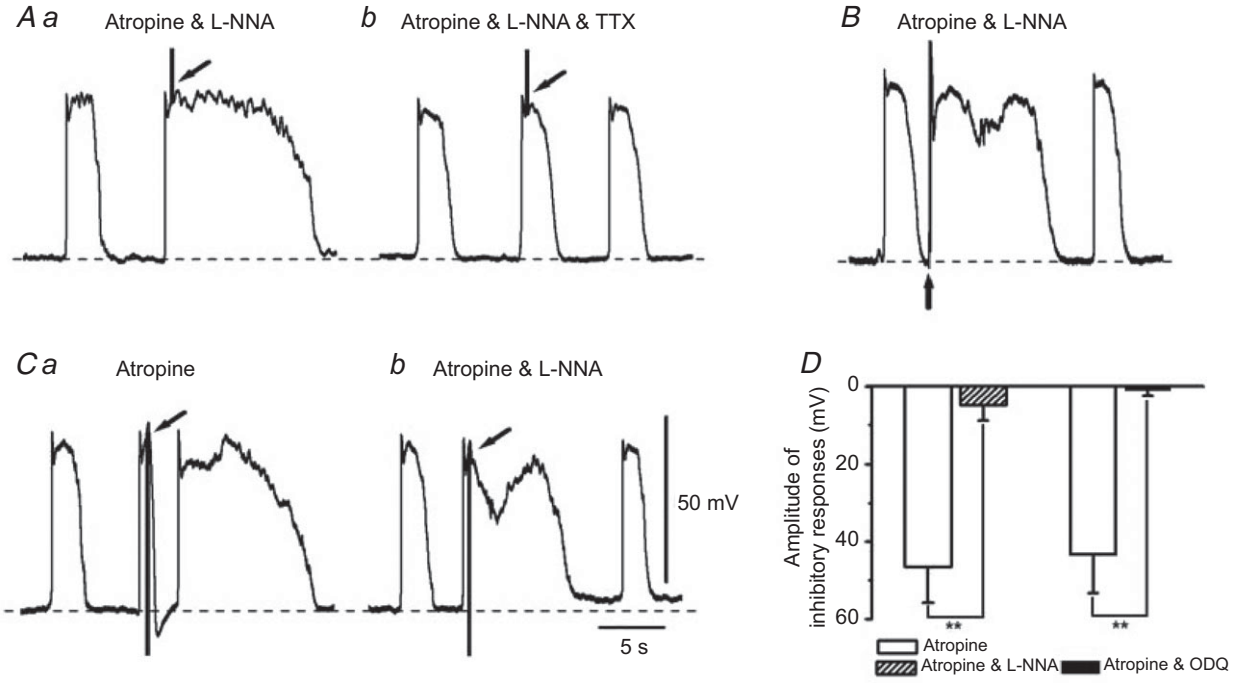

Figure 10. Properties of junction potentials evoked by electrical field stimulation recorded from ICC-MY of rabbit small intestine
A, EFS was applied at the peak of slow waves$_{ICC}$ in the presence of atropine (3 μM) and L-NNA (100 μM) (*Aa*) and after application of 1 μM TTX (*Ab*). *B*, EFS was applied during the intervals between slow waves$_{ICC}$ in the presence of atropine (3 μM) and L-NNA (100 μM). *C*, IJPs were evoked at the peak of slow waves$_{ICC}$ before (*Ca*) and after application of 100 μM L-NNA (*Cb*). Atropine (3 μM) was present throughout. *D*, summary of the effects of L-NNA (100 μM) or ODQ (10 μM) on IJPs evoked at the peak of slow waves$_{ICC}$ recorded from ICC-MY in the presence of atropine. Scale bars on the electrical traces in *C* apply to all traces. The resting membrane potentials were: *A*, −66 mV; *B*, −65 mV; *C*, −64 mV. *A*, *B* and *C* were recorded from different tissues. Data are means ± SD. $^{**}P < 0.01$, significant difference from control.

with dye injection into impaled cells: (1) spindle-shaped cells with slow waves lying within the longitudinal layer, (2) spindle-shaped cells with slow waves lying within the circular layer, (3) multipolar cells with triangular cell bodies with large amplitude slow waves between the two muscle layers and (4) irregular-shaped cells with several processes and STHs that occurred during slow waves or during the intervals between slow waves. The first and second types of cells were identified as LSMCs and CSMCs, respectively. The third type of cells were likely to be ICC-MY because of their morphological features and the fact that large amplitude slow waves were recorded from these cells, as has been observed in ICC-MY of the mouse small intestine (Kito & Suzuki, 2003). The fourth type of cell was distinguished from ICC-MY based on their cell shapes and the continuous discharge of STHs, which have never been detected in ICC-MY (Kito & Suzuki, 2003, 2007). We were unable to identify this fourth class of cells due to the poor reactivity of antibodies in rabbits to proteins known to be expressed by ICC or FLCs in other species. Therefore, the fourth class of cells with ongoing STHs was identified by electrophysiological behaviour that suggested these cells were FLCs.

An important finding in the present study is that the fourth class of cells impaled generates ongoing STHs in the rabbit small intestine and these events are conducted to SMCs in both the circular and the longitudinal muscle layers. STHs did not correlate with slow wave activity and were observed during the period between slow waves or at any point during the slow wave cycle. It has been reported that the amplitude of evoked and spontaneous IJPs was markedly reduced during spontaneous cyclical depolarizations (myoelectric complexes, MCs) in the circular muscle layer of mouse colon (Spencer *et al.* 1998). The authors demonstrated that there was a substantial attenuation or blockade of spontaneous and evoked transmitter release during the rising phase of each cyclical MC. Whilst the occurrence of STHs is similar to spontaneous IJPs in the circular muscle layer of mouse colon, it appears that the STHs are not due to periodic suppression of transmitter release because the STHs increased in amplitude as the membrane depolarized during each slow wave (Fig. 4*C*). Cells with STHs were located between the longitudinal and circular muscle layers because these cells were always impaled just after microelectrodes were advanced past the area where LSMCs were impaled and before impalements of CSMCs occurred. STHs were inhibited by MRS2500, a highly selective P2Y1 antagonist, and blocked by apamin. Previous studies have shown that P2Y1 receptors and SK3 channels are expressed mainly by FLCs in GI muscles (Kurahashi *et al.* 2011; Peri *et al.* 2013). Taken together, our data suggest that the fourth class of cells impaled in the intestinal muscles were FLCs (PDGFRα^+-MY cells), which have been shown to occupy the same anatomical region as the fourth class of cells impaled, express P2Y1 receptors and generate spontaneous transient outward currents that could underlie STHs (Kurahashi *et al.* 2011).

STHs with far smaller amplitudes were observed in LSMCs or CSMCs (Fig. 8). STHs detected in SMCs could result from the electronic spread of STHs from FLCs to smooth muscle layers, as SMCs are likely to be electrically coupled to FLCs via gap junctions, as reported previously in the mouse small intestine (Horiguchi & Komuro, 2000). Given that the amplitudes of STHs were larger in LSMCs than in CSMCs, it is possible that STHs regulate the excitability of LSMCs more effectively than CSMCs. It has been reported that Ca^{2+} spikes are superimposed on slow waves in LSMCs of rabbit small intestine under physiological conditions (Cheung & Daniel, 1980). Therefore, the main function of STHs in LSMCs may be to modulate the frequency of Ca^{2+} spikes by reducing the excitability of this muscle layer. The spontaneous electrical activities recorded from LSMCs or CSMCs of the rabbit small intestine consist of electrotonic cyclical depolarizations (slow waves) conducted from ICC-MY and small amplitude STHs probably conducted from FLCs, indicating that the three cell types are joined in an electrical syncytium. Thus, rabbit small intestinal smooth muscle preparations may be the ideal model for studying the spontaneous electrical activity of SMCs/ICC/PDGFRα^+ cell (SIP) syncytium, as recently proposed (Sanders *et al.* 2012).

Tonic inhibitory input to the GI tract has been observed in previous studies (Wood, 1972; Waterman & Costa, 1994; Spencer *et al.* 1998) and it is possible that STHs were, in part, due to input from purinergic neurotransmission. β-NAD and ATP have been shown to be released from colonic muscles spontaneously and during nerve stimulation (Hwang et al. 2012). Although both β-NAD and ATP caused hyperpolarization by activation of SK channels, only β-NAD-induced hyperpolarizations were blocked by MRS2500 (Mutafova-Yambolieva *et al.* 2007; Hwang *et al.* 2012). Therefore, it is possible that STHs were generated by β-NAD released from enteric inhibitory neurons. In this context, periodic alteration in the activity of STHs as shows in Fig. 5 may be the result of periodical activation of inhibitory motor neurons and release of β-NAD, which activate SK channels via P2Y1 receptors. STHs were abolished by apamin, but only reduced by MRS2500. Thus, generation of STHs may also occur by spontaneous activation of SK channels without stimulation by a purine neurotransmitter. Apamin-sensitive spontaneous transient outward currents (STOCs) were recorded previously from isolated PDGFRα^+ cells (Kurahashi *et al.* 2011).

As discussed in the previous paragraph the activation pattern of STHs suggests both intrinsic activation of SK channels in FLCs and activation by purine

neurotransmitters. Recent studies of FLCs (PDGFRα^+ cells) in gastric muscles showed that spontaneous Ca^{2+} waves were characteristic of these cells (Baker *et al.* 2013). Addition of purines greatly increased the frequency and amplitude of Ca^{2+} waves, and these effects were mediated by P2Y1 receptors and release of Ca^{2+} from intracellular stores. These data show that spontaneous Ca^{2+} release events could drive STHs in cells, and these events can be enhanced by purinergic stimulation.

Purinergic inhibitory responses were also observed as fIJPs in CSMCs of the rabbit small intestine. Unlike the different effects of MRS2500 and apamin on STHs recorded from FLCs, MRS2500 and apamin exerted similar inhibitory effects on fIJPs evoked in CSMCs. Thus, fIJPs are likely to result from a single pathway: release of a purine neurotransmitter, binding to P2Y1 receptors and activation of SK channels. It has been reported that in the deep muscular plexus (DMP) layer of the mouse small intestine, SK3 channel proteins are expressed in PDGFRα^+-DMP, but not by either CSMCs or ICC-DMP (Fujita *et al.* 2003; Iino *et al.* 2009). A recent study has shown that PDGFRα^+ cells isolated from the murine colon express P2Y1 receptors (Kurahashi *et al.* 2011). Therefore, it may be that purines released from purinergic neurons bind to P2Y1 receptors expressed in PDGFRα^+-DMP to cause fIJPs by the activation of SK3 channels in the rabbit small intestine. However, further studies are required to elucidate the role of PDGFRα^+-DMP in the generation of fIJPs in the rabbit small intestine.

Purinergic inhibitory responses were not observed in ICC-MY of the rabbit small intestine. This may be due to the absence of functional purinergic innervation in ICC-MY. An alternative explanation is that purinergic inhibitory nerves have little ability to alter the pacemaker activity of ICC-MY because of the lack of molecular and ionic apparatus to mediate purinergic responses in ICC-MY. Others found SK3 immunoreactivity in FLCs, but not in ICC-MY (Klemm & Lang, 2002; Vanderwinden *et al.* 2002; Fujita *et al.* 2003; Iino & Nojyo, 2009). Instead of inhibitory responses, EFS applied at the plateau component of slow waves$_{ICC}$ produced atropine-insensitive excitatory responses (increase the duration of slow waves$_{ICC}$) that were abolished by TTX. These results indicate that excitatory non-adrenergic, non-cholinergic nerves may innervate ICC-MY. Application of EFS during the intervals between slow waves$_{ICC}$ evoked a rapid depolarization. The same results were obtained in SMCs in the presence of atropine, L-NNA and MRS2500 (Fig. 9*A*). Thus, it is plausible that EJP-like responses in SMCs under these conditions reflect the depolarizations induced by EFS in ICC-MY. Unexpectedly, EFS at the plateau component of slow waves$_{ICC}$ halted slow waves$_{ICC}$ by generating IJP-like inhibitory responses in the presence of atropine, which were inhibited by pretreatment of L-NNA or ODQ, suggesting that nitric oxide (NO) released by neurons causes IJP-like inhibitory responses via the formation of cyclic GMP in ICC-MY. These results indicate that nitrergic nerves may innervate ICC-MY in the rabbit small intestine. However, we cannot exclude the possibility that NO released from enteric motor nerves during the application of EFS affects pacemaker activity by simple overflow onto ICC-MY. In either case, these results provide evidence that pacemaker activity may be under nitrergic inhibitory control in the rabbit small intestine.

In conclusion, two types of cells with slow wave activity were identified electrophysiologically, which were morphologically confirmed to be LSMCs and CSMCs. Cells with pacemaker activity and STHs are likely to be ICC-MY and FLCs, respectively. STHs were generated by the activation of apamin-sensitive (SK) channels. STHs with small amplitudes were also detected in smooth muscle layers. Therefore, FLCs appear to have a role in regulating smooth muscle excitability in the rabbit small intestine by contributing transient hyperpolarizations. In addition, purinergic inhibitory neurotransmission regulates rabbit small intestinal motility by eliciting fIJPs.

References

Baker SA, Hennig GW, Salter AK, Kurahashi M, Ward SM & Sanders KM (2013). Distribution and Ca^{2+} signalling of fibroblast-like (PDGFR$^+$) cells in the murine gastric fundus. *J Physiol* **591**, 6193–6208.

Burns AJ, Lomax AE, Torihashi S, Sanders KM & Ward SM (1996). Interstitial cells of Cajal mediate inhibitory neurotransmission in the stomach. *Proc Natl Acad Sci U S A* **93**, 12008–12013.

Burns AJ (2007). Disorders of interstitial cells of Cajal. *J Pediatr Gastroenterol Nutr* **45**(Suppl 2), S103–S106.

Cajal SR (1911). *Histologie du systeme nerveux de l'homme et des vertebres*, **vol.2**, pp. 891–942. Maloine, Paris.

Cheung DW & Daniel EE (1980). Comparative study of the smooth muscle layers of the rabbit duodenum. *J Physiol* **309**, 13–27.

Cobine CA, Hennig GW, Kurahashi M, Sanders KM, Ward SM & Keef KD (2011). Relationship between interstitial cells of Cajal, fibroblast-like cells and inhibitory motor nerves in the internal anal sphincter. *Cell Tissue Res* **344**, 17–30.

Crist JR, He XD & Goyal RK (1992). Both ATP and the peptide VIP are inhibitory neurotransmitters in guinea-pig ileum circular muscle. *J Physiol* **447**, 119–131.

Dickens EJ, Edwards FR & Hirst GD (2000). Vagal inhibition in the antral region of guinea pig stomach. *Am J Physiol Gastrointest Liver Physiol* **279**, G388–G399.

Duffy AM, Cobine CA & Keef KD (2012). Changes in neuromuscular transmission in the *W/W^v* mouse internal anal sphincter. *Neurogastroenterol Motil* **24**, e41–e55.

Farrugia G (2008). Interstitial cells of Cajal in health and disease. *Neurogastroenterol Motil* **20**(Suppl 1), 54–63.

Fujita A, Takeuchi T, Jun H & Hata F (2003). Localization of Ca^{2+}-activated K^+ channel, SK3, in fibroblast-like cells forming gap junctions with smooth muscle cells in the mouse small intestine. *J Pharmacol Sci* **92**, 35–42.

Gabella G & Blundell D (1979). Nexuses between the smooth muscle cells of the guinea-pig ileum. *J Cell Biol* **82**, 239–247.

Gallego D, Vanden Berghe P, Farré R, Tack J & Jiménez M (2008). P2Y1 receptors mediate inhibitory neuromuscular transmission and enteric neuronal activation in small intestine. *Neurogastroenterol Motil* **20**, 159–168.

He XD & Goyal RK (1993). Nitric oxide involvement in the peptide VIP-associated inhibitory junction potential in the guinea-pig ileum. *J Physiol* **461**, 485–499.

Henderson RH, Duchon G & Daniel EE (1971). Cell contacts in duodenal smooth muscle layers. *Am J Physiol* **221**, 564–574.

Horiguchi K & Komuro T (2000). Ultrastructural observations of fibroblast-like cells forming gap junctions in the W/W^v mouse small intestine. *J Auton Nerv Syst* **80**, 142–147.

Huizinga JD, Thuneberg L, Kluppel M, Malysz J, Mikkelsen HB & Bernstein A (1995). W/*kit* gene required for interstitial cells of Cajal and for intestinal pacemaker activity. *Nature* **373**, 347–349.

Hwang SJ, Blair PJ, Durnin L, Mutafova-Yambolieva V, Sanders KM & Ward SM (2012). P2Y1 purinoreceptors are fundamental to inhibitory motor control of murine colonic excitability and transit. *J Physiol* **590**, 1957–1972.

Iino S, Horiguchi K, Horiguchi S & Nojyo Y (2009). c-Kit-negative fibroblast-like cells express platelet-derived growth factor receptor α in the murine gastrointestinal musculature. *Histochem Cell Biol* **131**, 691–702.

Iino S & Nojyo Y (2009). Immunohistochemical demonstration of c-Kit-negative fibroblast-like cells in murine gastrointestinal musculature. *Arch Histol Cytol* **72**, 107–115.

Kito Y & Suzuki H (2003). Properties of pacemaker potentials recorded from myenteric interstitial cells of Cajal distributed in the mouse small intestine. *J Physiol* **553**, 803–818.

Kito Y & Suzuki H (2007). Role of K^+ channels in the regulation of electrical spontaneous activity of the mouse small intestine. *Pflugers Arch* **455**, 505–514.

Kito Y, Sanders KM, Ward SM & Suzuki H (2009). Interstitial cells of Cajal generate spontaneous transient depolarizations in the rat gastric fundus. *Am J Physiol Gastrointest Liver Physiol* **297**, G814–G824.

Kito Y (2012). Spontaneous electrical activity of fibroblast-like cells. *Neurogastroenterol Motil* **24**(Suppl 2), WS-10, 002.

Klemm MF & Lang RJ (2002). Distribution of Ca^{2+}-activated K^+ channel (SK2 and SK3) immunoreactivity in intestinal smooth muscles of the guinea-pig. *Clin Exp Pharmacol Physiol* **29**, 18–25.

Komuro T, Seki K & Horiguchi K (1999). Ultrastructural characterization of the interstitial cells of Cajal. *Arch Histol Cytol* **62**, 295–316.

Komuro T (2006). Structure and organization of interstitial cells of Cajal in the gastrointestinal tract. *J Physiol* **576**, 653–658.

Kurahashi M, Zheng H, Dwyer L, Ward SM, Koh SD & Sanders KM (2011). A functional role for the 'fibroblast-like cells' in gastrointestinal smooth muscles. *J Physiol* **589**, 697–710.

Kurahashi M, Nakano Y, Hennig GW, Ward SM & Sanders KM (2012). Platelet-derived growth factor receptor-positive cells in the tunica muscularis of human colon. *J Cell Mol Med* **16**, 1397–1404.

Mutafova-Yambolieva VN, Hwang SJ, Hao X, Chen H, Zhu MX, Wood JD, Ward SM & Sanders KM (2007). β-Nicotinamide adenine dinucleotide is an inhibitory neurotransmitter in visceral smooth muscle. *Proc Natl Acad Sci U S A* **104**, 16359–16364.

Peri LE, Sanders KM & Mutafova-Yambolieva VN (2013). Differential expression of genes related to purinergic signaling in smooth muscle cells, PDGFRα-positive cells, and interstitial cells of Cajal in the murine colon. *Neurogastroenterol Motil* **25**, e609–e620.

Sanders KM & Ward SM (1992). Nitric oxide as a mediator of nonadrenergic, noncholinergic neurotransmission. *Am J Physiol* **262**, G379–G392.

Sanders KM (1996). A case for interstitial cells of Cajal as pacemakers and mediators of neurotransmission in the gastrointestinal tract. *Gastroenterology* **111**, 492–515.

Sanders KM, Ordog T, Koh SD, Torihashi S & Ward SM (1999). Development and plasticity of interstitial cells of Cajal. *Neurogastroenterol Motil* **11**, 311–338.

Sanders KM, Hwang SJ & Ward SM (2010). Neuroeffector apparatus in gastrointestinal smooth muscle organs. *J Physiol* **588**, 4621–4639.

Sanders KM, Koh SD, Ro S & Ward SM (2012). Regulation of gastrointestinal motility-insights from smooth muscle biology. *Nat Rev Gastroenterol Hepatol* **9**, 633–645.

Spencer NJ, Bywater RA & Taylor GS (1998). Disinhibition during myoelectric complexes in the mouse colon. *J Auton Nerv Syst* **71**, 37–47.

Stark ME, Bauer AJ & Szurszewski JH (1991). Effect of nitric oxide on circular muscle of the canine small intestine. *J Physiol* **444**, 743–761.

Suzuki H, Ward SM, Bayguinov YR, Edwards FR & Hirst GD (2003). Involvement of intramuscular interstitial cells in nitrergic inhibition in the mouse gastric antrum. *J Physiol* **546**, 751–763.

Thuneberg L (1982). Interstitial cells of Cajal: intestinal pacemaker cells? *Adv Anat Embryol Cell Biol* **71**, 1–130.

Vanderwinden JM & Rumessen JJ (1999). Interstitial cells of Cajal in human gut and gastrointestinal disease. *Microsc Res Tech* **47**, 344–360.

Vanderwinden JM, Rumessen JJ, de Kerchove d'Exaerde A Jr, Gillard K, Panthier JJ, de Laet MH & Schiffmann SN (2002). Kit-negative fibroblast-like cells expressing SK3, a Ca^{2+}-activated K^+ channel, in the gut musculature in health and disease. *Cell Tissue Res* **310**, 349–358.

Wang GD, Wang XY, Hu HZ, Liu S, Gao N, Fang X, Xia Y & Wood JD (2007). Inhibitory neuromuscular transmission mediated by the P2Y1 purinergic receptor in guinea pig small intestine. *Am J Physiol Gastrointest Liver Physiol* **292**, G1483–G1489.

Ward SM, Dalziel HH, Bradley ME, Buxton IL, Keef KD, Westfall DP & Sanders KM (1992). Involvement of cyclic GMP in non-adrenergic, non-cholinergic inhibitory neurotransmission in dog proximal colon. *Br J Pharmacol* **107**, 1075–1082.

Ward SM, Burns AJ, Torihashi S & Sanders KM (1994). Mutation of the proto-oncogene *c-kit* blocks development of interstitial cells and electrical rhythmicity in murine intestine. *J Physiol* **480**, 91–97.

Ward SM & Sanders KM (2006). Involvement of intramuscular interstitial cells of Cajal in neuroeffector transmission in the gastrointestinal tract. *J Physiol* **576**, 675–682.

Waterman SA & Costa M (1994). The role of enteric inhibitory motoneurons in peristalsis in the isolated guinea-pig small intestine. *J Physiol* **477**, 459–468.

Wood JD (1972). Excitation of intestinal muscle by atropine, tetrodotoxin, and xylocaine. *Am J Physiol* **222**, 118–125.

Additional information

Competing interests

The authors declare no conflicts of interests.

Acknowledgements

This project was supported by the 24th General Assembly of the Japanese Association of Medical Sciences to Y.K.

Author contributions

Conception and design of the experiments: Y.K. Collection, analysis and interpretation of data: Y.K., M.K., R.M., S.M.W. and K.M.S. Drafting the article or revising it critically for important intellectual content: Y.K., S.M.W. and K.M.S. All authors read and approved the manuscript for submission.